Open Veterinary Journal, (2023), Vol. 13(1): 1–10
ISSN: 2226-4485 (Print)
ISSN: 2218-6050 (Online)

Original Research
DOI: *10.5455/OVJ.2023.v13.i1.1*

Submitted: 28/09/2022 Accepted: 06/12/2022 Published: 03/01/2023

Histomorphometry and µCT scan analysis of osteoporosis in spayed female dogs

Ernest Kostenko[1*], Alius Pockevičius[2], and Algirdas Maknickas[1]

[1]*Department of Biomechanical Engineering, Vilnius Gediminas Technical University, Vilnius, Lithuania*
[2]*Department of Veterinary Pathobiology, Lithuanian University of Health Sciences, Kaunas, Lithuania*

Abstract

Background: Both humans and small animals suffer from similar metabolic and structural diseases that impact the musculoskeletal system; however, instead of studying animal disease in its own right, animals are more often used as models for research into various human ailments, such as osteoporosis. There are few studies indicating that animals may suffer from osteoporosis, which raises the question of why small animals, which we believe to be equally susceptible, receive so little attention. With this research, we hope to draw the attention of researchers to the fact that the examination of animals for this disease is just as important as the examination of humans; human osteoporosis research receives a great deal of attention, while animals and their health are neglected.

Aims: We aimed to analyze the bone volume fraction (BV/TV) and thickness of first (L1) and second (L2) lumbar vertebrae samples from five cadavers using histomorphometric analysis. In addition, we aimed to investigate one cadaver using microcomputed tomography (µCT) imaging.

Methods: The L1 and L2 vertebrae from five dog carcasses were used to evaluate the BV/TV and the trabecular thicknesses. We used precise sampling criteria, and also developed a methodological approach to the study of the vertebrae. Using semi-automated methods, we performed histomorphometric analysis and µCT data analysis.

Results: We used five dog cadavers in this research. During the histomorphometry study, we observed that the lowest L1 BV/TV ratio was 7.88% and the highest was 23.08%. The L2 vertebrae BV/TV ranged from 11.58% to 23.7%. The L1 and L2 lumbar trabeculae thicknesses were also measured. L1's smallest trabecula was 17.34 microns and its largest was 31.88. The L2 vertebrae trabecula thickness was 18.76–30.75 microns. BV/TV and trabecular thickness were positively correlated (and vice versa). The two-tailed *p* value was less than 0.00001. This difference is statistically significant. After µCT analysis, we discovered regions in the vertebral body with low porosity; these cavities are usually filled with connective tissue. The bone tissue in these areas is more vulnerable, meaning fracture risk has increased.

Conclusions: Animals should not just be considered as models for osteoporosis in humans, but also as potential patients. A single test, such as histomorphometry, may not be sufficient; more advanced technology, such as µCT, is required, since it reveals the pores that make the vertebral column more brittle and susceptible to fracture.

Keywords: Canine, Osteoporosis, Histomorphometry, Microcomputed tomography.

Introduction

For the study of osteoporosis, scientists have used histopathological samples for many years, since this study method allows to comprehend the pathophysiology of the disease, draws conclusions, and prescribes the proper treatment or make other recommendations. However, after reviewing the scientific literature, we discovered that the study of osteoporosis in animals receives very little attention, while in humans, osteoporosis has been extensively studied, as it is considered a global disease (Maistrovskaia *et al*., 2022). In the scientific literature, animals are exclusively used as models for the study of human disease. The scientific literature typically describes rats as the gold standard for osteoporosis research (Jee and Yao, 2001; Banu, 2011; Popović *et al*., 2016). However, larger animals, such as sheep, can also be used (Turner, 2001, 2002; Zarrinkalam *et al*., 2009), and it is possible to investigate rabbits, dogs, and other larger animals (Reinwald and Burr, 2008; Kaveh, 2010; Reinwald and Burr, 2011). The mechanical qualities of the spine have a significant impact on the development of the disease; in our most recent publication, we analyzed the mechanical properties of canine lumbar vertebrae (Kostenko *et al*., 2022a, 2022b).

Adopting a method reduces the possibility of errors (Fig. 1). We chose to examine the canine spine because this species is owned by a large proportion of the world's population, and dogs are particularly valuable for elderly people (Keat *et al*., 2016).

***Corresponding Author:** Ernest Kostenko. Department of Biomechanical Engineering, Vilnius Gediminas Technical University, Vilnius, Lithuania. Email: *Ernest.kostenko@vilniustech.lt*

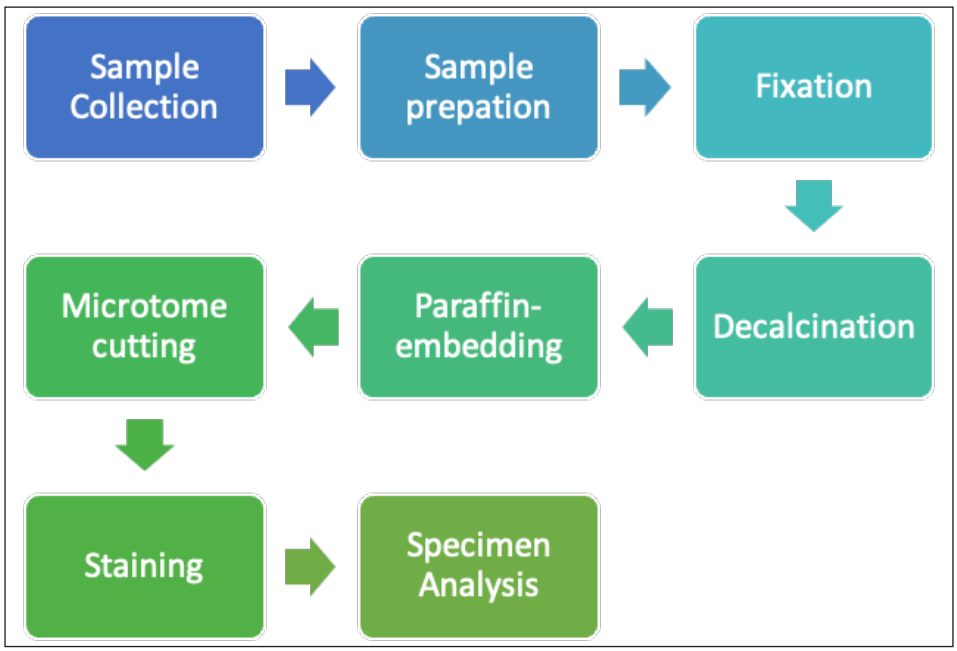

Fig. 1. Investigation protocol.

In this article, we aimed to investigate whether companion animals like dogs are also susceptible to this sickness and whether research should be undertaken to find this disorder in these animals as well. To test our hypothesis, histomorphometry was chosen, because it provides a high-resolution 2D analysis of bone mass and architecture. Regardless of bone mass, histomorphometry accurately evaluates the bone structure and detects bone fragility (Lelovas *et al*., 2008). Its most interesting feature is its ability to assess numerous characteristics, which are categorized as static, dynamic, and structural (Kulak and Dempster, 2010). We also used microcomputed tomography (μCT), because this enabled us to study small samples in greater detail. μCT has been designed to study extremely small samples or examine small structural elements such as the trabeculae present in bone tissue. The greatest advantage of this technique is that high-resolution images can be obtained.

Materials and Methods

Table 1 gives the details of which animal carcasses were chosen. The average age was 10.2 ± 2.8 years; the average weight was 16.72 ± 4.03 kg. Three dogs were purebred and two were of mixed breed.

Sampling required a strict protocol. The most important steps were to collect samples of canine lumbar vertebrae devoid of musculoskeletal defects of average-sized, spayed dogs and to complete a consent form (Table 2). To avoid involving live animals in our experiment, we used animal carcasses. All animals used had terminal diseases and were euthanized by good veterinary practice, and all necessary consents were obtained.

Histology sample preparation technique

We collected a total of 11 vertebrae samples: 6 second lumbar vertebrae (L2) and 5 first lumbar vertebrae (L1). During necropsy, the lumbar segments were removed and were then split to prepare the sample. We utilized a band saw to cut the vertebrae samples (MAINCA, Spain) (Medina-Serra *et al*., 2021).

A 10% neutrally buffered formalin solution was used for sample fixation (Sigma Aldrich, USA.).

Next, we decalcified samples with a DC1 histological decalcifier (WWR Chemicals, France) (Miquelestorena-Standley *et al*., 2020).

To remove the formalin from the histology samples, they were trimmed, placed in cassettes, and rinsed with cold tap water.

Once the formalin was removed, the cassettes containing the samples were placed in a tissue processor (Thermo Scientific Shandon Pathcenter, Fisher Scientific, USA) (Bemenderfer *et al*., 2014), where tissue dehydration was performed with increasing concentrations of ethanol (60%, 80%, and 96% alcohol) and isopropyl alcohol (Baskin, 2014). Using an embedding center (Tes 99 Paraffin Embedding Center, Medite, Germany) (Birkenfeld *et al*., 2019), samples were cleared with chloroform and flushed with xylene, then embedded in paraffin.

To make histology slides, paraffin-embedded samples were cut into 4-μm thick sections with Leica 818 high-profile microtome blades using a microtome (Leica RM2235, Leica Biosystems, Germany) (Mohamad *et al.*, 2021). Sections were submerged in water at 37°C before being placed on glass slides and dried on a heating plate. The slides were then stained with

Table 1. Examined carcasses.

Age, years	13	10	13	7	8
Breed	Border collie	French bulldog	Mixed breed	Mixed breed	Chow Chow
Reproductive status	Ovariectomized	Ovariectomized	Ovariectomized	Ovariectomized	Ovariectomized
Weight, kg	21.0	13.2	12.9	15.5	21.0

Table 2. Sample collection guidelines.

Animal species	Canine
Gender	Female
Weight	15–25 kg
Age	Non-specific
Reproductive status	Spayed
Breed	Non-specific
Body mass index	Poor or average
Muscle development	No
Joint damage	Doesn't matter (if the present must be evaluated)
Anamnesis	The experimental animals should not have metabolic diseases, thyroid diseases, or rickets, osteomalacia, osteomyelitis, bone tumors, osteochondritis, dysplasia, spinal hernia, disc spondylosis or discospondylitis, and fixed bone fracture. If there is a fixed bone fracture unless the required bone samples are damaged.
Required bones	Lumbar vertebrae (L1 and L2)

haematoxylin and eosin using an automatic staining system (Tissue-Tek DRS™, Sakura, Japan) (Botolin *et al*., 2005). Sample staining allows for the differentiation of many structural components, such as trabeculae, cartilage tissue, bone tissue, and other tissue elements (Dettmeyer, 2018). The stained slides were then covered with cover slip and coated with a mounting medium (Thermo Scientific Shandon Consul-Mount™ Histology Formulation, Thermo Scientific, USA) (Filipowska *et al*., 2017).

Histological samples were evaluated using an Olympus BX63 microscope and Olympus DP72 microscope camera equipped with Olympus cell-Sens Dimension software (Olympus, Japan).

Evaluation of bone tissue using the histomorphometry technique

The nomenclature was created by Parfitt *et al.* (1987) and later modified and enhanced by Dempster *et al.* (2013) (Table 3). When performing bone histomorphometry analysis, it is crucial to comprehend the meaning of the numerous indexes which can be obtained (Table 4).

We only studied static parameters because they are of utmost importance in determining the risk for vertebral fracture.

To get a comprehensive histological image of the sample, we had to merge all views into a single image using the Olympus Cell-Sens Dimension software (Fig. 2).

For our research and measurements, we used open-source software Osteohisto (van't Hof *et al*., 2017), which allowed us to determine the structural properties of our samples.

We began by measuring the entire sample surface area, followed by the total trabecular surface area. We determined the bone volume fraction (BV/TV) of the vertebrae by dividing the bone trabecular area by the total sample area and multiplying by 100 (Fig. 3). Using the same software, we were also able to calculate the perimeter (Pm) of the entire bone tissue and the ratio of bone surface to bone volume (BS/BV) (Table 5).

Evaluation of bone tissue using the µCT technique

We only performed µCT on a single sample of the spine, since we have extremely limited access to this technology in our country. µCT imaging of the lumbar vertebrae of dogs confirmed that osteoporosis is also present in animals. The equipment specifications are shown in Table 6. The Nikon XT H 225 universal entry-level system has a micro-focused X-ray source, an inspection volume suitable for tiny to medium-sized items, and high picture quality. The XT H 225 is appropriate for various applications, including the inspection of plastic components, tiny castings, and intricate mechanisms, as well as the investigation of materials and natural specimens like vertebrae. During data acquisition, the Nikon XT H 225 CT scanner with microfocus maintains fixed positions, while the plate on which the CT-scanned item rests is slowly rotated 360 degrees. A projection picture of the sample is cast on a 45 × 45 cm^2 Perkin Elmer detector panel with a matrix of 2,048 × 2,048 pixels for each angle increment

Table 3. List of abbreviations.

Name	Abb.
Area	Ar
Bone	B
Tissue	T
Trabecula(r)	Tb
Thickness	Th
Total	Tt
Volume	V
Width	Wi
Bone surface	BS
Bone volume	BV
Tissue volume	TV
Perimeter	Pm

Table 4. List of structural parameters.

Name of index	Abb.	Formula
Trabecular number	Tb. N	(BV/TV)/TB.Th
Trabecular separation	Tb. Sp	(1/Tb.N)-Tb. Th
Trabecular width	Tb. Wi	(BV/TV)Tb. Th

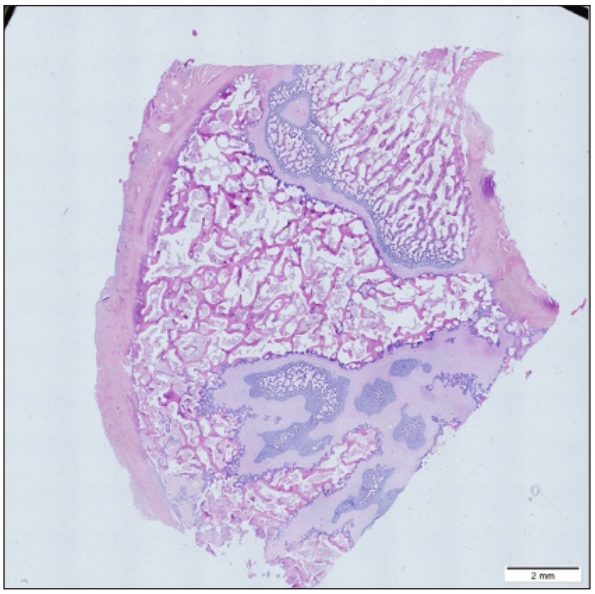

Fig. 2. Merged histopathology sample.

(Beaulieu and Dutilleul, 2019). We used Osirix MD software to analyze the obtained data.

Ethical approval

All bioethical and animal welfare standards were adhered to according to Regulation (EC) No 1069/2009 of the European Parliament and of the Council of October 21, 2009 and Regulation (EC No 1774/2002 (animal by-products regulation) and the Lithuanian Law on Welfare and Protection of Animals.

Results

Histomorphometry

Different L1 and L2 vertebral parameters were investigated (Fig. 4). The lowest BV/TV ratio of a L1 vertebra was 7.88% and the highest was 23.08%. In the study of L2 vertebrae, the lowest BV/TV was 11.58% and the highest was 23.7%.

The thickness of the trabeculae in the L1 and L2 lumbar vertebrae was also assessed independently. The smallest trabecula in L1 measured 17.34 microns and the biggest measured 31.88 microns. The L2 vertebrae had a minimum trabecula thickness of 18.76 microns and a maximum of 30.75 microns (Fig. 5). If trabeculae are damaged or crushed in, they will be able to withstand a much smaller load and so have a greater likelihood of breaking.

There was a considerable positive association between BV/TV and trabecular thickness (and vice versa), as seen in Figure 6: the two-tailed p value was less than 0.00001. According to established statistical criteria, this difference is deemed to be highly significant.

µCT scan

Using X-ray imaging, every volumetric element of the sample, not just its surface contour, was digitized. We obtained almost 24 GB of data, which required specialized software for its analysis. The trabeculae in the vertebral body can be seen clearly in Figure 7. After analyzing the different sections, we discovered that there are locations in the vertebral body where porosity is very high, and it is reasonable to assume that these cavities are filled with connective tissue. The bone tissue in these locations is more fragile; there has been a change in the bone structure, and there would be an increased fracture risk.

Discussion

In the evaluation of bone tissue, the application of µCT as well as histomorphometric analysis might be of great assistance (Gielkens *et al*., 2008). There are standards for detecting osteoporosis in humans, the dual-energy x-ray absorptiometry (DXA) scan being the gold standard (Touban *et al*., 2022). However, it is vital to keep in mind that bone BV/TV can vary from case to case, depending on a variety of factors, including hormones, but also lifestyle behavior, level of physical activity, and medication usage. Research that examined lumbar vertebrae and evaluated BV/TV and cortical thickness in the lumbar vertebrae has demonstrated this. These two parameters are especially important for assessing osteoporosis (Maknickas *et al*., 2019). A study that examined healthy individuals with osteoporosis likewise examined vertebrae, but the resultant BV/TV was different (Zupan *et al*., 2013). Table 7 shows a comparison table using data acquired by other author Yoshida *et al*. (1998) and our data.

Significance of trabeculae and fracture risk

Trabecular (cancellous) bone is the primary component of a bone; it is organized in packets to form a connected,

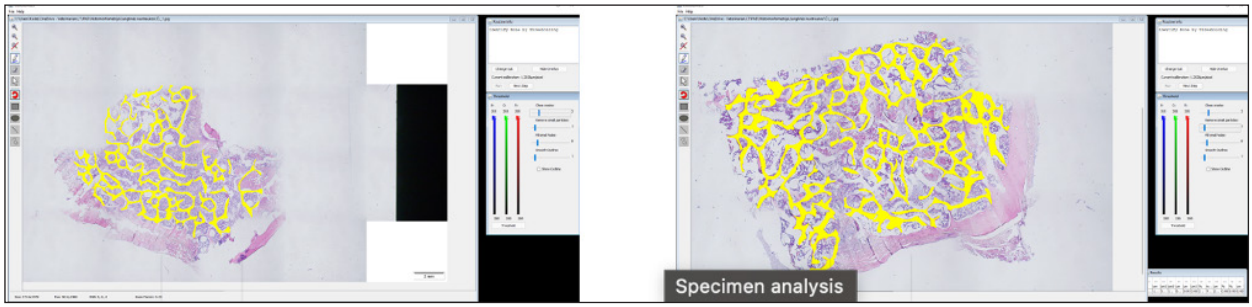

Fig. 3. (a) L1 bone density evaluation and (b) L2 bone density evaluation.

Table 5. Analysis sample data obtained using OsteoidHisto.

Sample name	Calibration, µm	T.Ar, µm²	B.Ar µm²	BV/TV, %	BS/BV, mm⁻¹	Tb.Th, µm
CL_L1	1.2928	5,416,102.92	1,137,322.93	21	70.64	28.31
CL_L2	1.2928	5,803,098.13	1,375,051.5	23.7	69.25	28.88
Mil_L1	1.2928	1,881,386.5	433,944.6	23.07	66.13	30.24
Mil_L2	1.2928	5,316,680.4	615,740.38	11.58	95.31	20.98
ML_L2	1.2928	5,543,752.56	1,031,681.39	18.61	78.98	25.32
RL_L1	1.2928	5,917,741.47	466,034.17	7.88	101.57	19.69
RL_L2	1.2928	6,100,205.78	1,020,160.9	16.72	65.04	30.75
S21002_L1	1.2928	1,644,587.19	310,003.64	18.85	62.74	31.88
S21002_L2	1.2928	5,935,206.89	902,688	15.21	77.42	25.83
SL_L1	1.2928	4,798,903.47	471,365.72	9.82	115.35	17.34
SL_L2	1.2928	6,933,384.76	914,392.33	13.19	106.62	18.76
				0.32	0.17	1.24

Standard deviation (SD) (van't Hof *et al*., 2017).

Table 6. µCT equipment characteristics.

Equipment used	Nikon XT H 225
Accuracy	Up to 7 microns (µm)
Technique	A point source of X-rays and a 14-bit detector with 7.5 million pixels
Voxel dimensions	0.05 × 0.05 × 0.05 mm
Sample height	38 mm
Sample length	486 mm
Radiation	127 kV; 90 microamperes
Obtained data	24 GB

irregular array of plates and rods known as trabeculae. The thickness of these trabeculae ranges anywhere from 100 to 200 microns on average, with the exact value depending on the anatomic region as well as the age of the donor in humans (Keaveny, 1998). Cancellous bone resistance to compressive loads is a characteristic of great theoretical and practical therapeutic value. Diseases such as osteoporosis have a significant impact on the structure of human trabecular bone, which leads to a variety of adverse effects including an increased risk of fractures (Anam *et al*., 2021). For the use of internal prostheses and skeletal fixation in humans and companion animals, it is necessary to have knowledge about fractures of normal and osteoporotic bone and disorders that affect skeletal metabolism (Galante *et al.*, 1970). Before surgery, an orthopedic traumatologist must always conduct a fracture risk assessment. Particular consideration should be given to the animal's age, sex, and reproductive state, as well as its nutrition. Currently, there are no specialized risk assessment criteria or techniques for estimating fracture risk in animals, similar to the fracture risk assessment

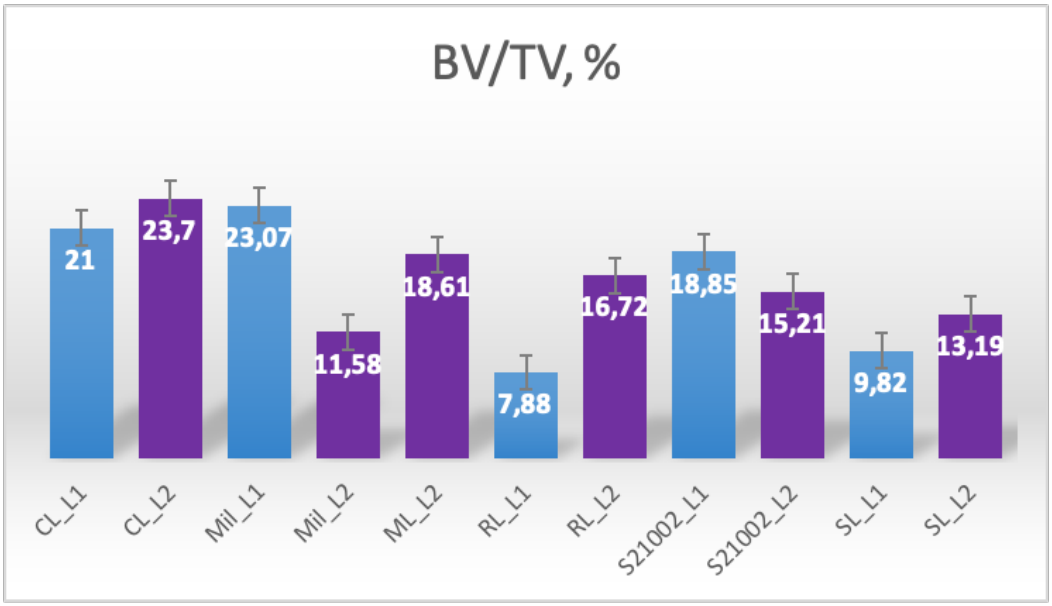

Fig. 4. Bone volume fraction.

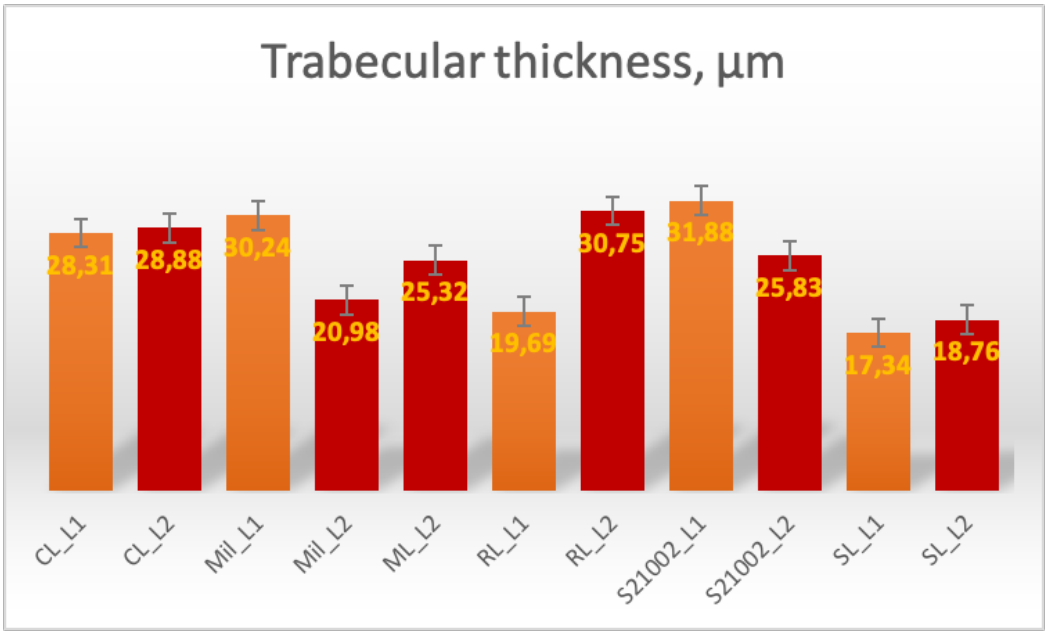

Fig. 5. Trabecular thickness.

and prediction tools available for humans. One of the principal tools is known as FRAX and is frequently utilized in human medicine (Kanis *et al*., 2008).

Previous investigation into the trabecular bone structure has been based on morphometric examination of histological sections (Parkinson and Fazzalari, 2013). Because of this, we decided to investigate the bone tissue using histomorphometry. To increase the reliability of the results, we also performed µCT on one sample. Non-destructive X-ray imaging techniques, such as µCT, have allowed imaging of the three-dimensional structure of the trabecular bone measurements (Parkinson and Fazzalari, 2013).

Features of the biomechanics of the quadruped lumbar spine

Canine and human spine and spinal components are comparable. Both species have similar intervertebral discs and facet joints. Humans have 33 vertebrae, and dogs have 50. Dogs have 13 thoracic and 7 lumbar vertebrae, while humans have 12 thoracic and 5 lumbar vertebrae (Fingeroth and Thomas, 2015). However, humans are bipeds, whereas dogs are quadrupeds.

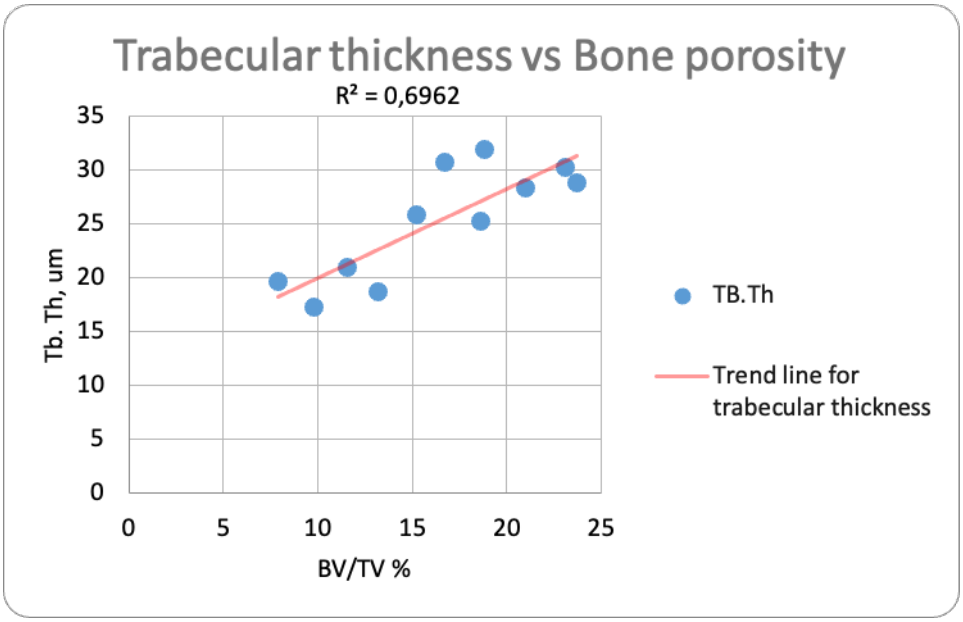

Fig. 6. Correlation between trabecular thickness and BV/TV.

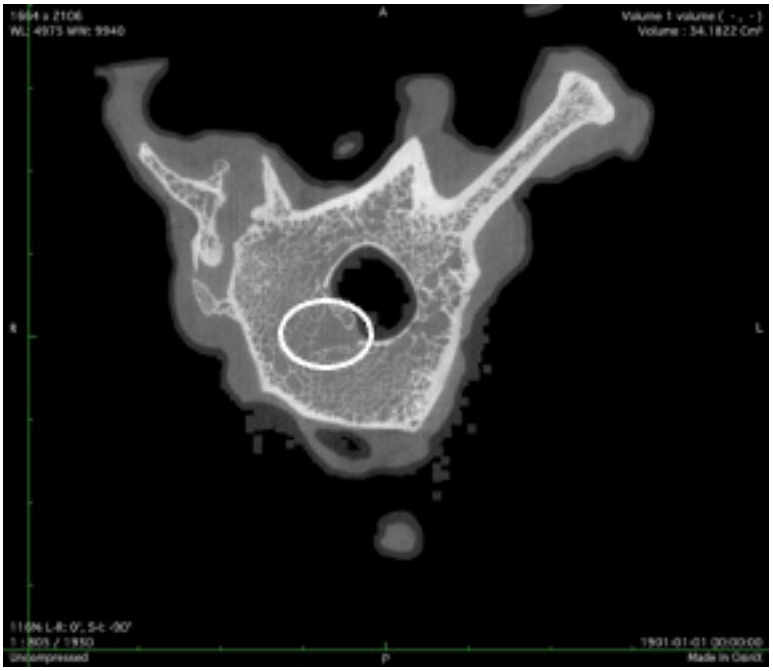

Fig. 7. Visible defects in the canine L2 vertebra.

Consequently, the architecture and biomechanics of the canine spine may differ from those of humans. The highest load on the human spine is applied by the vertebral bodies, whereas the greatest load in animals is applied by the spinous processes. Vertebrae in canines can withstand considerable compression. According to Wolff's law, the trabecular structure of cortical bone responds to compressive pressure by strengthening. As with the human spine, the quadruped spine appears to be loaded by axial compression (Smit, 2002).

Estrogen deficiency

No remnants of the ovaries were found. Female dogs usually come into heat once or twice a year, and their sex cycle is different from mice or humans. Lack of hormones is not only a factor that can increase bone porosity; other risk factors, such as excessive use of steroid anti-inflammatory drugs, dietary habits, and lack of physical activity can also have a significant impact. Numerous research papers have examined the advantages of spaying; for example, in one study,

Table 7. Comparison of BV/TV thickness and trabeculae in the lumbar spine of dogs.

	Our results	OVX canine (Yoshida *et al*., 1998)	Non-OVX canine (Yoshida *et al*., 1998)
BV/TV, %	16.33 ± 5.3	15.3 ± 1.2	21.2 ± 2.2
Tb. Th, μm	25.27 ± 5.25	83.3 ± 3.9	92.6 ± 4.6

spayed female canines older than 10 years were found to have a significantly reduced risk of pyometra (Egenvall *et al*., 2001). Another finding was a considerable reduction in the number of mammary gland tumors in spayed female dogs (Gilbertson *et al*., 1983).

Consideration must be given to the negative effects of hormone withdrawal, which can lead to reproductive, locomotor, urinary, metabolic, and other illnesses, as described in Urfer and Kaeberlein's (2019) review. Martin *et al*. (1987) discovered that, 11 months after ovariectomy was performed, the volume of trabecular bone in beagle vertebrae was significantly reduced, but there were no notable changes in the cortical bone. Another study by Yoshida *et al*. (1998) examined the efficacy of osteoporosis therapy in spayed female beagles and found that BV/TV and trabecular thickness differed considerably between spayed and non-spayed dogs. One more study of spayed female canines revealed that the lack of ovarian hormones had no significant effect on cortical bone remodeling activity and that the loss of ovarian function might have a more pronounced effect on trabecular bone than on cortical bone (Snow *et al.*, 1984).

Unfortunately, dogs are not the best model for researching estrogen-deficient bone. To examine the effect of estrogen on bone tissue, it is important to quantify the estrogen levels in the serum of spayed and intact female dogs (Martin *et al*., 1987). Nonetheless, dogs are very good models for investigating fracture healing, the effects of immobility, the long-term impacts of particular bone-forming chemicals, bone growth, and joint replacement (Turner, 2001).

With this study, we hope to draw the attention of scientists to the fact that companion animals, such as dogs, may develop osteoporosis, even though this disease has received little attention in companion animals.

Conclusion

Animals are studied as models for osteoporosis in people, but humans are not the only species affected by this condition. Animals should also be seen as potential osteoporosis patients.

It is possible that a single examination, such as histomorphometry, will not be sufficient; in that case, more advanced techniques, such as μCT, could be additionally used. Using this technique, we detected holes in the vertebral body that were caused by osteoporosis.

We anticipate that, with decreased BV/TV and a decrease in the size of the trabeculae, the trabeculae would be able to sustain less external force. μCT reveals the pores that cause the vertebral column to be more fragile and susceptible to breaking.

More samples are required for more accurate results that would allow us to investigate the factors associated present in these animals.

Author contributions

The study was co-authored by all authors. The final manuscript was read and approved by all authors.

Conflict of interest

The authors declare that there is no conflict of interest.

References

Anam, M., Hussain, M., Nadeem, M.W., Javed Awan, M., Goh, H.G. and Qadeer, S. 2021. Osteoporosis prediction for trabecular bone using machine learning: a review. Comput. Mater. Contin. 67(1), 89–105.

Banu, J. 2011. The ovariectomized mice and rats. In Osteoporosis research. London, UK: Springer, pp: 101–114.

Baskin, D.G. 2014. Fixation and tissue processing in immunohistochemistry. Pathobiology of human disease. San Diego, CA: Elsevier, pp: 3797–3806.

Beaulieu, J. and Dutilleul, P. 2019. Applications of computed tomography (CT) scanning technology in forest research: a timely update and review. Can. J. Forest Res. 49(10), 1173–1188.

Bemenderfer, T.B., Harris, J.S., Condon, K.W. and Kacena, M.A. 2014. Tips and techniques for processing and sectioning undecalcified murine bone specimens. In Skeletal development and repair. Totowa, NJ: Humana Press, pp: 123–147.

Birkenfeld, F., Sengebusch, A., Völschow, C., Möller, B., Naujokat, H. and Wiltfang, J., 2019. Scaffold implantation in the omentum majus of rabbits for new bone formation. J. Cranio-Maxillofac. Surg. 47(8), 1274–1279.

Botolin, S., Faugere, M.C., Malluche, H., Orth, M., Meyer, R. and McCabe, L.R. 2005. Increased bone adiposity and peroxisomal proliferator-activated receptor-γ2 expression in type I diabetic mice. Endocrinology 146(8), 3622–3631.

Dempster, D.W., Compston, J.E., Drezner, M.K., Glorieux, F.H., Kanis, J.A., Malluche, H., Meunier, P.J., Ott, S.M., Recker, R.R. and Parfitt, A.M. 2013. Standardized nomenclature, symbols, and units for bone histomorphometry: a 2012 update of the report of the ASBMR Histomorphometry Nomenclature Committee. J. Bone Miner. Res. 28(1), 2–17.

Dettmeyer, R.B., 2018. Staining techniques and microscopy. In Forensic histopathology. Cham, Switzerland: Springer, pp: 17–45.

Egenvall, A., Hagman, R., Bonnett, B.N., Hedhammar, A., Olson, P. and Lagerstedt, A.S. 2001. Breed risk of pyometra in insured dogs in Sweden. J. Vet. Int. Med. 15(6), 530–538.

Filipowska, J., Cholewa-Kowalska, K., Wieczorek, J., Semik, D., Dąbrowski, Z., Łączka, M. and Osyczka, A.M. 2017. Ectopic bone formation by gel-derived bioactive glass-poly-L-lactide-co-glycolide composites in a rabbit muscle model. Biomed. Mater. 12(1), 015015.

Fingeroth, J. and Thomas, W. Eds. 2015. Advances in intervertebral disc disease in dogs and cats. Oxford, UK: John Wiley & Sons.

Galante, J., Rostoker, W. and Ray, R.D. 1970. Physical properties of trabecular bone. Calcified Tiss. Res. 5(1), 236-246.

Gielkens, P.F., Schortinghuis, J., de Jong, J.R., Huysmans, M.C.D., van Leeuwen, M.B.M., Raghoebar, G.M., Bos, R.R. and Stegenga, B. 2008. A comparison of micro-CT, microradiography and histomorphometry in bone research. Arch. Oral Biol. 53(6), 558–566.

Gilbertson, S.R., Kurzman, I.D., Zachrau, R.E., Hurvitz, A.I. and Black, M.M. 1983. Canine mammary epithelial neoplasms: biologic implications of morphologic characteristics assessed in 232 dogs. Vet. Pathol. 20(2), 127–142.

Jee, W.S. and Yao, W. 2001. Overview: animal models of osteopenia and osteoporosis. J. Musculoskelet. Neuronal. Interact. 1(3), 193–207.

Kanis, J.A., McCloskey, E.V., Johansson, H., Strom, O., Borgstrom, F. and Odén, A. 2008. Case finding for the management of osteoporosis with FRAX®—assessment and intervention thresholds for the UK. Osteopor. Inter. 19(10), 1395–1408.

Kaveh, K., Ibrahim, R., Abubakar, M.Z. and Ibrahim, T.A. 2010. Osteoporosis induction in animal model. Am. J. Anim. Vet. Sci. 5(2), 139–145.

Keat, K.C., Subramaniam, P., Ghazali, S.E. and Amit, N., 2016. Review on benefits of owning companion dogs among older adults. Mediterr. J. Soc. Sci. 7(4), 397–397.

Keaveny, T.M. 1998. Cancellous bone. In Handbook of biomaterial properties. Eds., Black, J. and Hastings, G. New York, NY: Springer.

Kostenko, E., Pockevičius, A. and Maknickas, A. 2022a. Histomorphometric analysis of canine trabecular bone in the osteoporotic context. In ESB 2022: 27th Congress of the European Society of Biomechanics, 2022 Jun 26–29, European Society of Biomechanics, Porto, Portugal.

Kostenko, E., Stonkus, R., Šengaut, J. and Maknickas, A. 2022b. Empirical case report of the mechanical properties of three spayed canine lumbar vertebrae. Open Vet. J. 12(3), 414–425.

Kulak, C.A.M. and Dempster, D.W. 2010. Bone histomorphometry: a concise review for endocrinologists and clinicians. Arq. Bras. Endocrinol. Metabol. 54, 87–98.

Lelovas, P.P., Xanthos, T.T., Thoma, S.E., Lyritis, G.P. and Dontas, I.A. 2008. The laboratory rat as an animal model for osteoporosis research. Comp. Med. 58(5), 424–430.

Maistrovskaia, Y.V., Nevzorova, V.A., Ugay, L.G., Gnedenkov, S.V., Kotsurbei, E.A., Moltyh, E.A., Kostiv, R.E. and Sinebryukhov, S.L. 2022. Bone tissue condition during osteosynthesis of a femoral shaft fracture using biodegradable magnesium implants with an anticorrosive coating in rats with experimental osteoporosis. Appl. Sci. 12(9), 4617.

Maknickas, A., Alekna, V., Ardatov, O., Chabarova, O., Zabulionis, D., Tamulaitienė, M. and Kačianauskas, R. 2019. Fem-based compression fracture risk assessment in osteoporotic lumbar vertebra l1. Appl. Sci. 9(15), 3013.

Martin, R.B., Butcher, R.L., Sherwood, L.L., Buckendahl, P., Boyd, R.D., Farris, D., Sharkey, N. and Dannucci, G. 1987. Effects of ovariectomy in beagle dogs. Bone 8(1), 23-31.

Medina-Serra, R., Foster, A., Plested, M., Sanchis, S., Gil-Cano, F. and Viscasillas, J. 2021. Lumbar erector spinae plane block: an anatomical and dye distribution evaluation of two ultrasound-guided approaches in canine cadavers. Vet. Anaesth. Analg. 48(1), 125–133.

Miquelestorena-Standley, E., Jourdan, M.L., Collin, C., Bouvier, C., Larousserie, F., Aubert, S., Gomez-Brouchet, A., Guinebretière, J.M., Tallegas, M., Brulin, B. and Le Nail, L.R., 2020. Effect of decalcification protocols on immunohistochemistry and molecular analyses of bone samples. Mod. Pathol. 33(8), 1505–1517.

Mohamad, N.V., Ima-Nirwana, S. and Chin, K.Y. 2021. Self-emulsified annatto tocotrienol improves bone histomorphometric parameters in a rat model of oestrogen deficiency through suppression of skeletal sclerostin level and RANKL/OPG ratio. Int. J. Med. Sci. 18(16), 3665.

Parfitt, A.M., Drezner, M.K., Glorieux, F.H., Kanis, J.A., Malluche, H., Meunier, P.J., Ott, S.M. and Recker, R.R. 1987. Bone histomorphometry: standardization of nomenclature, symbols, and units: report of the ASBMR Histomorphometry Nomenclature Committee. J. Bone Miner. Res. 2(6), 595–610.

Parkinson, I.H. and Fazzalari, N.L. 2013. Characterisation of trabecular bone structure. In Skeletal aging and osteoporosis. Berlin, Heidelberg, Germany: Springer, pp: 31–51.

Popović, T., Šrbić, R., Matavulj, M., Obradović, Z. and Sibinčić, S. 2016. Experimental model of osteoporosis on 14 weeks old ovariectomised rats: biochemical, histological and biomechanical study. Biol. Serbica 38(1), 18–27.

Reinwald, S. and Burr, D. 2008. Review of nonprimate, large animal models for osteoporosis research. J. Bone Miner. Res. 23(9), 1353–1368.

Reinwald, S. and Burr, D.B. 2011. Other large animal models. In Osteoporosis research. London, UK: Springer, pp: 159–174.

Smit, T.H. 2002. The use of a quadruped as an in vivo model for the study of the spine–biomechanical considerations. Eur. Spine J. 11(2), 137–144.

Snow, G.R., Cook, M.A. and Anderson, C. 1984. Oophorectomy and cortical bone remodeling in the beagle. Calcif. Tissue Int. 36(1), 586–590.

Touban, B.M., Sayegh, M.J., Galina, J., Pavlesen, S., Radwan, T. and Anders, M. 2022. Computed tomography measured psoas cross sectional area is associated with bone mineral density measured by dual energy X-ray absorptiometry. J. Clin. Densitom. 25(4), 592–598.

Turner, A.S. 2001. Animal models of osteoporosis-necessity and limitations. Eur. Cell Mater. 1(66–81), 13.

Turner, A.S. 2002. The sheep as a model for osteoporosis in humans. Vet. J. 163(3), 232–239.

Urfer, S.R. and Kaeberlein, M. 2019. Desexing dogs: a review of the current literature. Animals 9(12), 1086.

van't Hof, R.J., Rose, L., Bassonga, E. and Daroszewska, A. 2017. Open source software for semi-automated histomorphometry of bone resorption and formation parameters. Bone 99, 69–79.

Yoshida, Y., Moriya, A., Kitamura, K., Inazu, M., Okimoto, N., Okazaki, Y. and Nakamura, T. 1998. Responses of trabecular and cortical bone turnover and bone mass and strength to bisphosphonate YH529 in ovariohysterectomized beagles with calcium restriction. J. Bone Miner. Res. 13(6), 1011–1022.

Zarrinkalam, M.R., Beard, H., Schultz, C.G. and Moore, R.J. 2009. Validation of the sheep as a large animal model for the study of vertebral osteoporosis. Eur. Spine J. 18(2), 244–253.

Zupan, J., van't Hof, R.J., Vindišar, F., Haring, G., Trebše, R., Komadina, R. and Marc, J. 2013. Osteoarthritic versus osteoporotic bone and intra-skeletal variations in normal bone: Evaluation with μCT and bone histomorphometry. J. Orthop. Res. 31(7), 1059–1066.